



HAL
open science

TGFBI secreted by mesenchymal stromal cells ameliorates osteoarthritis and is detected in extracellular vesicles

Maxime Ruiz, Karine Toupet, Marie Maumus, Pauline Rozier, Christian Jorgensen, Danièle Noël

► To cite this version:

Maxime Ruiz, Karine Toupet, Marie Maumus, Pauline Rozier, Christian Jorgensen, et al.. TGFBI secreted by mesenchymal stromal cells ameliorates osteoarthritis and is detected in extracellular vesicles. *Biomaterials*, 2020, 226, pp.119544. 10.1016/j.biomaterials.2019.119544 . hal-02329519

HAL Id: hal-02329519

<https://hal.umontpellier.fr/hal-02329519>

Submitted on 23 Oct 2019

HAL is a multi-disciplinary open access archive for the deposit and dissemination of scientific research documents, whether they are published or not. The documents may come from teaching and research institutions in France or abroad, or from public or private research centers.

L'archive ouverte pluridisciplinaire **HAL**, est destinée au dépôt et à la diffusion de documents scientifiques de niveau recherche, publiés ou non, émanant des établissements d'enseignement et de recherche français ou étrangers, des laboratoires publics ou privés.

1
2
3
4 TGFBI secreted by mesenchymal stem cells ameliorates
5
6
7
8 osteoarthritis and is detected in extracellular vesicles
9

10
11
12
13
14
15 Maxime Ruiz^a, Karine Toupet^a, Marie Maumus^a, Pauline Rozier^a, Christian

16
17
18 Jorgensen^{a,b,*}, Danièle Noël^{a,b,*}
19
20
21
22

23 ^aIRMB, Univ Montpellier, INSERM, CHU Montpellier, Montpellier, France; ^bHôpital Lapeyronie,

24
25
26 Clinical immunology and osteoarticular diseases Therapeutic Unit, Montpellier, France.
27
28

29 *: equally contributing authors
30
31
32
33
34
35
36
37
38
39
40
41
42
43
44
45

46
47 *Corresponding author:*
48

49 D. Noël, Inserm U1183, IRMB, Hôpital Saint-Eloi,

50
51
52 80 avenue Augustin Fliche, 34295 Montpellier cedex 5, France
53

54 Tel: +33 4 67 33 04 73 – Fax: +33 4 67 33 01 13 – E-mail: daniele.noel@inserm.fr
55
56
57
58
59
60
61
62
63
64
65

1
2
3
4 **ABSTRACT**
5

6 Mesenchymal stem/stromal cells (MSCs) are of interest in the context of osteoarthritis (OA)
7 therapy. We previously demonstrated that TGF β -induced gene product-h3 (TGFB1/BIGH3) is
8 downregulated in human MSCs (hMSCs) from patients with OA, suggesting a possible link with
9 their impaired regenerative potential. In this study, we investigated TGFB1 contribution to MSC-
10 based therapy in OA models. First, we showed that co-culture with murine MSCs (mMSCs) partly
11 restored the expression of anabolic markers and decreased expression of catabolic markers in
12 OA-like chondrocytes only upon priming by TGF β 3. Moreover, TGF β 3-primed hMSCs not only
13 modulated the expression of anabolic and catabolic markers, but also decreased inflammatory
14 factors. Then, we found that upon TGFB1 silencing, mMSCs partly lost their inductive effect on
15 chondrocyte anabolic markers. Injection of hMSCs in which TGFB1 was silenced did not protect
16 mice from OA development. Finally, we showed that MSC chondroprotection was due to the
17 presence of TGFB1 mRNA and protein in extracellular vesicles. Our findings suggest that TGFB1 is
18 a chondroprotective factor released by MSCs and an anabolic regulator of cartilage
19 homeostasis.
20
21
22
23
24
25
26
27
28
29
30
31
32
33
34
35
36
37
38
39
40
41
42
43
44
45
46
47
48
49

50 **Keywords:** mesenchymal stem cells, TGFB1, osteoarthritis, cartilage, chondrocyte, extracellular
51 vesicle
52
53
54
55
56
57
58
59
60
61
62
63
64
65

INTRODUCTION

Mesenchymal stem/stromal cells (MSCs) are multipotent progenitor cells that are primarily isolated from bone marrow and adipose tissue, but that can also be found in many other tissues, including umbilical cord and deciduous teeth [1]. These fibroblastic-like adherent cells are characterized by a panel of positive and negative markers and the potential to differentiate into the three mesenchymal lineages [2]. MSCs also secrete many factors that act in a paracrine fashion and play important roles in their therapeutic effect [3]. Recent findings indicate that most of these factors are conveyed by extracellular vesicles (EVs) that take part in intercellular communication by acting as vehicles for the transfer of mediators between cells [4]. Previous studies on factors that mediate *in vivo* the beneficial function of MSCs showed that interleukin 6 (IL6), IL1 receptor antagonist, and glucocorticoid induced leucine zipper are anti-inflammatory mediators in experimental arthritis, whereas thrombospondin-1 is a chondroprotective factor in osteoarthritis (OA) [5-8]. Nevertheless, the identification of factors responsible for MSC clinical benefit in rheumatic diseases is still incomplete.

OA is the most common rheumatic disease. Its prevalence increases with age, and is higher in patients with metabolic syndromes or obesity [9]. OA is characterized by progressive cartilage destruction, but it also affects all other joint tissues, leading to sub-chondral bone sclerosis, synovium inflammation and fat pad fibrosis [10, 11]. In patients with severe forms, it results in the loss of joint function, pain and functional disability. Currently, there is no curative treatment and the available pharmaceutical options only alleviate symptoms, such as pain and inflammation. In patients with advanced OA, joint replacement surgery offers pain relief and restores function and mobility. Recent studies have evaluated the interest of delivering MSCs in

1
2
3
4 the pathological joint, as a possible innovative therapeutic solution. MSC chondroprotective
5
6 effect has been demonstrated in preclinical models of OA [12-14], and the safety and efficacy of
7
8 this approach are now evaluated in the clinic (for review, see [15]). Both allogeneic and
9
10 autologous MSCs are used; however, questions have been raised on the efficacy of MSCs
11
12 isolated from aged donors or with age-associated diseases [16]. Indeed, MSCs from aged donors
13
14 show reduced proliferative capacity, differentiation potential, and migration as well as
15
16 increased senescence [17]. As MSCs adapt and respond to their microenvironment, a
17
18 pathological state might perturb the stem cell niche where MSCs reside. Therefore, the
19
20 interactions between MSCs and their niche will result in modifications of their secretome. For
21
22 instance, several factors secreted in the joint environment, particularly members of the
23
24 transforming growth factor- β (TGF β) family [18], are deregulated in OA and contribute to the
25
26 breakdown of cartilage homeostasis. At basal levels, TGF β signalling contributes to cartilage
27
28 homeostasis. On the other hand, high concentrations of TGF β are found in the synovial fluids of
29
30 patients with OA [19]. Interestingly, deregulation of TGF β signalling in MSCs is involved in OA
31
32 onset or progression, and knock out of TGF β type II receptor in MSCs attenuates cartilage
33
34 erosion and subchondral bone sclerosis [20]. We recently reported that TGF β -induced gene
35
36 product-h3 (TGFBI/BIGH3/RGD-CAP) is upregulated in cartilage and bone from patients with OA,
37
38 whereas it is downregulated in bone marrow-derived human MSCs (hMSCs) [21]. We also found
39
40 that TGFBI downregulation in hMSCs partly compromises their chondrogenic potential.
41
42 Therefore, we hypothesized that TGFBI downregulation in hMSCs from patients with OA may
43
44 affect their functional properties and impair their regenerative/repair potential. Here, we
45
46 investigated whether TGFBI deregulation in OA affects MSC chondroprotective role.
47
48
49
50
51
52
53
54
55
56
57
58
59
60
61
62
63
64
65

MATERIALS AND METHODS

Mesenchymal stem cell culture. Human specimens were recovered from patients with OA undergoing knee replacement surgery after written informed consent, in accordance with the Declaration of Helsinki. The study was carried out following the recommendations by the Languedoc-Roussillon Committee for the Protection of Persons and was approved by the French Ministry of Higher Education and Research (DC-2010-1185). After isolation from bone marrow, hMSCs were characterized by phenotyping and tri-lineage differentiation, as described [22]. They were cultured in proliferative medium [α MEM, 2 mmol/mL glutamine, 100 μ g/mL penicillin/streptomycin, 10% foetal calf serum (FCS), and 1 ng/mL basic fibroblast growth factor (bFGF) (R&D Systems, Lille)], and used between passage 2 and 5. Murine MSCs (mMSCs) were isolated from bone marrow of C57BL/6 mice, expanded in proliferative medium, and characterized as previously reported [5]. They were used between passage 12 and 20.

EV isolation and characterization. EVs were isolated from conditioned supernatants of mMSCs (mMSC-EVs) by differential ultracentrifugation to recover large-size EVs and small-size EVs at 18 000 and 100 000 g, respectively. EVs were characterized following the guidelines provided by the International Society of Extracellular Vesicles (ISEV), as already described in [23]. Similar protocols were used for the production and isolation of hMSC-EVs. Briefly, hMSCs (10^6 /dish) were cultured in proliferative medium with 3% EV-free FCS for 60h for production of EV-rich supernatant. Total EVs, which contain small-size and large-size EVs, were isolated according to the described protocol [23]. EV characterization included the determination of size

1
2
3
4 and concentration by nanoparticle tracking analysis (NanoSight LM10-12 Malvern Instruments,
5
6 Orsay), protein quantification with the Micro BCA Protein Assay Kit (Pierce, ThermoFisher
7
8 Scientific, Illkirsch), and surface marker detection (anti-CD81 from Miltenyi Biotech, Paris; and
9
10 anti-CD44, -CD63, CD73, -CD90, -CD105 antibodies from BD Biosciences, Le Pont de Claix) on EV-
11
12 coated beads, as described [23].
13
14
15
16
17
18
19

20 **Cartilage explant and chondrocyte culture.** Femoral heads were dissected from 2-week-old
21
22 C57BL/6 mice as described [24]. After 72h of stabilization in proliferative medium, OA-like
23
24 changes were induced in cartilage explants by culture in serum-free medium with 10 ng/mL IL-
25
26 1 β (R&D Systems) for another 72h. Thereafter, OA-like explants were co-cultured with 2×10^5
27
28 mMSCs seeded in polyethylene terephthalate culture inserts with 0.4 μ m pore size (BD, Corning,
29
30 Boulogne-Billancourt) for 24h.
31
32
33
34

35 Murine articular chondrocytes were isolated from the knees and femoral heads of 3-day-
36
37 old C57BL/6 mice, as described [25]. Chondrocytes were plated ($25\ 000\ \text{cells}/\text{cm}^2$) in 12-well TPP
38
39 culture plates (TPP Techno Plastic Products, Switzerland) with 1mL of proliferative medium for 5
40
41 days. Thereafter, OA-like chondrocytes were induced by incubation with 1 ng/mL IL-1 β (R&D
42
43 Systems) for 24h (day 0). In parallel, mMSCs were cultured in 1mL of proliferative medium in 12-
44
45 well culture plates. At 80% confluence, they were primed (or not) with 10 ng/mL TGF β 3 (R&D
46
47 Systems) for 24h, then rinsed twice with PBS, and cultured for 24h to obtain conditioned
48
49 medium (mMSC-CM). mMSC-CM (1mL/well) was then added to OA-like chondrocytes for 24h
50
51 (day 1) before recovering chondrocytes for RT-qPCR analysis.
52
53
54
55
56
57
58
59
60
61
62
63
64
65

1
2
3
4 For co-culture with mMSCs or hMSCs, 2×10^5 OA-like chondrocytes were seeded in 12-well
5
6 culture inserts with 1mL of proliferative medium and primed (or not) with 10 ng/mL TGF β 3 for
7
8 24h. After two washes with PBS, mMSC- or hMSC-containing inserts were added to OA-like
9
10 chondrocytes on day 0 with fresh medium and co-cultured for 24h (day 1). Chondrocytes were
11
12 recovered and processed for RT-qPCR.
13
14
15
16
17
18
19

20 **Glycosaminoglycan (GAG) content measurement.** GAG content was measured using the
21
22 Blyscan Glycosaminoglycan Assay according to the supplier's recommendations (Biocolor Ltd,
23
24 UK). Supernatants from OA-like explants were collected and cultured OA-like explants were
25
26 digested overnight with 125 μ g/mL papain (Sigma) in sodium acetate buffer (0.1M; pH=5.5)
27
28 containing 5mM EDTA and 5mM L-cysteine HCl. Supernatants and digestion products were
29
30 diluted to fit the calibration curve. Colorimetric values were obtained using a Varioskan LUX
31
32 microplate reader.
33
34
35
36
37
38
39

40 **Cell transfections.** At 60% confluence, mMSCs and hMSCs were transfected with 50nM of
41
42 siRNA-control (siCT), siRNA-mTGFB1 or siRNA-hTGFB1 (siTGFB1) (Ambion, ThermoFisher Scientific)
43
44 using the Oligofectamine reagent and according to the supplier's recommendations (Life
45
46 Technologies, Courtaboeuf). Chondrocytes were transfected with 400nM of each siRNA using
47
48 the Lipofectamine reagent, according to the supplier's recommendations (Life Technologies,
49
50 Courtaboeuf). Cells were used 48h after transfection.
51
52
53
54
55
56
57
58
59
60
61
62
63
64
65

1
2
3
4 **Proliferation and adhesion assays.** For both assays, 96-well TPP plates were coated with
5
6 10 µg/mL recombinant human TGFBI (rhTGFBI; R&D Systems) and incubated at 4°C overnight.
7
8 Then, wells were washed twice with PBS and blocked with 2% BSA at room temperature for 1h.
9
10 For proliferation assays, 2×10^4 murine chondrocytes were seeded on rhTGFBI-coated plates and
11
12 incubated for 72h. For adhesion assays, 5×10^4 murine chondrocytes were seeded on rhTGFBI-
13
14 coated plates and after 2h, 4h, and 6h, wells were washed twice with PBS to remove non-
15
16 adherent cells before quantification of the adhering cells. Cell number was quantified by
17
18 measuring cell viability using the CellTiter-Glo luminescent assay (Promega, Charbonnières-les-
19
20 Bains), according to the manufacturer's protocol. Cell numbers were estimated relative to a
21
22 standard curve generated using 10-fold serial dilutions of chondrocytes and the cell number in
23
24 non-treated wells was set to 1.
25
26
27
28
29
30
31
32
33
34

35 **Splenocyte proliferative assay.** Splenocytes were isolated from C57Bl6 mice and cultured
36
37 with hMSCs transfected with siCT or siTGFBI, as described [8]. After 3 days of incubation,
38
39 splenocyte proliferation was assessed using the CellTiter-Glo Luminescent Cell Viability Assay
40
41 (Promega, Charbonnières-les-Bains) following the manufacturer's instructions. Splenocyte
42
43 proliferation was quantified by subtracting the signal of unstimulated splenocytes, and
44
45 calculated as the percentage of the value obtained in concanavalin A-stimulated splenocytes
46
47 (100%).
48
49
50
51
52
53
54
55

56 **RNA extraction and RT-qPCR.** Total RNA was isolated from h/mMSCs or chondrocytes using
57
58 the RNeasy kit according to the supplier's protocol (Qiagen, Courtaboeuf); from cartilage and
59
60
61
62
63
64
65

1
2
3
4 bone with 0.1 mL TRIzol reagent (ThermoFisher Scientific)/g tissue, followed by chloroform and
5
6 phenol acid extraction; and from EVs using the miRNeasy Micro Kit (Qiagen). Total RNA (0.5 µg)
7
8 was reverse transcribed using 100 U of M-MLV reverse transcriptase (ThermoFisher Scientific),
9
10 and PCR reactions were performed as described [26]. Primer sequences (SYBR Green
11
12 Technologies) are described in Table 1. All values were normalized to the *RPS9* housekeeping
13
14 gene, and expressed as relative expression or fold change using the respective formulae: $2^{-\Delta CT}$
15
16 and $2^{-\Delta\Delta Ct}$. For EVs, gene expression was quantified in 10 ng of cDNA and normalized to the Ct
17
18 values.
19
20
21
22
23
24
25
26

27 **Collagenase-induced osteoarthritis model.** The collagenase-induced OA (CIOA) model was
28
29 generated in accordance with the guidelines and regulations of the Ethical Committee for
30
31 animal experimentation of the Languedoc-Roussillon region (Approval APAFIS#5349-
32
33 2016050918198875). Experiments were performed after the final approval by the French
34
35 Ministry for Education, Higher Education and Research. OA was induced by two injections (day 0
36
37 and 2) of 1U type VII collagenase in 5 µL saline in the intra-articular (IA) space of one hind knee
38
39 joint in 10-week-old C57BL/6 mice. Then, groups of 23 mice received or not IA injections of siCT-
40
41 or siTGFB1-transfected hMSCs (2.5×10^5 cells/5 µL saline) at day 7. Mice were euthanatized at day
42
43 42 and hind paws were fixed in 4% formaldehyde for further analysis.
44
45
46
47
48
49
50
51
52

53 **Bone parameter analysis.** Hind paws were scanned in a SkyScan 1176 micro-CT scanner
54
55 (Bruker, Belgium) using the following parameters: 0.5 mm aluminium filter, 45 kV, 500 µA,
56
57 resolution of 18 µm, 0.5° rotation angle. Scans were reconstructed using the NRecon software
58
59
60
61
62
63
64
65

1
2
3
4 (Bruker). Misalignment compensation, ring artefacts and beam-hardening were adjusted to
5
6 obtain the correct reconstruction of each paw. Bone degradation was quantified in subchondral
7
8 bone of the medial plateau for each tibia (CTAn software, Bruker). Calcification of the lateral
9
10 and medial meniscal/external ligaments and osteophyte formation on joint edges were also
11
12 quantified. 3D images of joints were reconstructed using the Avizo software (Avizo Lite 9.3.0, FEI
13
14 Visualization Sciences Group, Lyon, France).
15
16
17
18
19
20
21

22 **Confocal laser scanning microscopy.** A confocal laser scanning microscope (CLSM; TCS SP5-
23
24 II, Leica Microsystems, Nanterre) was used to acquire images of the medial tibial plateau
25
26 articular cartilage. Articular cartilage was scanned in depth (XYZ-mode) using the following
27
28 parameters: voxel size 6 μm , 5x dry objective, and UV laser light source (405 nm). Image stacks
29
30 were used to reconstruct a 3D image of the medial tibial plateau cartilage and then to quantify
31
32 cartilage morphometric parameters using the Avizo software.
33
34
35
36
37
38
39

40 **Histological analysis.** Hind paws were decalcified in 5% formic acid solution for 2 weeks,
41
42 and then processed for paraffin embedding. Coronal sections of tibias were cut (3 slices of 7 μm
43
44 each 100 μm ; first section at 50 μm below the cartilage surface) and stained with Safranin
45
46 O/Fast Green. Cartilage degradation was quantified using the modified Pritzker OARSI score, as
47
48 described [27]. Osteophyte size at the edges of the tibia cartilage was scored using an arbitrary
49
50 score from 0 to 3, as described [14].
51
52
53
54
55
56
57
58
59
60
61
62
63
64
65

1
2
3
4 **Statistical analysis.** Statistical analysis was performed with the GraphPad Prism software.

5
6 Each sample/cell was independent and represented an experimental unit providing a single
7
8 outcome. The data normal distribution and variance homogeneity were determined with the
9
10 Shapiro-Wilk and Fisher's exact tests (2 groups) or the Bartlett's test (>2 groups), followed by
11
12 the appropriate tests, as detailed in each figure legend. Data are presented as the mean \pm SEM
13
14 with $p < 0.05$ (*), $p < 0.01$ (**), $p < 0.001$ (***).
15
16
17
18
19
20
21

22 **RESULTS**

23
24
25
26
27 **TGFBI is deregulated in OA-like femoral head explants and chondrocytes.** We previously
28
29 showed by immunohistochemistry that TGFBI is upregulated in the cartilage from patients with
30
31 OA and in CIOA mice compared with healthy controls [28]. To better understand the effect of
32
33 TGFBI deregulation, we first evaluated its expression by RT-qPCR in mice at different ages. We
34
35 found that *TGFBI* mRNA expression was higher in cartilage than in cortical bone or bone marrow
36
37 in healthy 3-day-old mice (Fig. 1A). *TGFBI* expression was also higher in the femoral heads of
38
39 adult mice compared with cortical bone or total bone marrow, and in tibial epiphyses compared
40
41 with bone marrow (Fig. 1B). This suggests higher expression in cartilage-containing tissues.
42
43 Importantly, *TGFBI* mRNA levels tended to be higher in tibial epiphyses from CIOA mice than in
44
45 healthy controls, confirming TGFBI upregulation in OA joint tissues (Fig. 1C). We next
46
47 determined whether OA-related TGFBI deregulation can be reproduced in *in vitro* models. First,
48
49 we demonstrated that mouse femoral head explants (Fig. 1D) cultured with IL1 β reproduced the
50
51 OA-like cartilage phenotype, as indicated by the downregulation of the anabolic markers
52
53
54
55
56
57
58
59
60
61
62
63
64
65

1
2
3
4 type IIB collagen (*Col2a1*) and aggrecan (*Acan*) and the upregulation of the catabolic markers
5
6 matrix metalloproteinase 13 (*Mmp13*) and A Disintegrin And Metalloproteinase with
7
8 Thrombospondin Motifs 5 (*Adamts5*) (Fig. 1E). In addition, IL1 β significantly increased GAG
9
10 release in the culture supernatant, and decreased GAG content in cartilage explants. Moreover,
11
12
13
14 *Tgfbi* level was higher in OA-like explants compared with untreated controls (Fig. 1E).

15
16
17 Similarly, immature articular chondrocytes isolated from neonatal mice displayed an OA-
18
19 like phenotype after incubation with IL1 β (Fig. 1F). Specifically, expression of *Col2a1* and *Acan*
20
21 was decreased, whereas that of *Mmp13* and *Adamts5* was increased after 24h of incubation
22
23 with IL1 β (Fig. 1G). Moreover, the genes encoding several inflammatory mediators, such as IL6,
24
25 inducible nitric oxide synthase (iNOS), monocyte chemoattractant protein (MCP)1 and
26
27 cyclooxygenase (COX)2, were upregulated, whereas tumour necrosis factor (TNF) α remained
28
29 unchanged. In this model, *Tgfbi* was downregulated (Fig. 1G), indicating a deregulation of TGFBI
30
31 in both *in vitro* models of OA.
32
33
34
35
36
37
38
39

40 **Naive murine and human MSCs cannot normalize the phenotype of OA-like chondrocytes.**

41
42 We then investigated the effect of mMSCs on OA-like femoral head explants (experimental
43
44 strategy in Fig. 1D). GAG release in the supernatant was decreased and the expression of *Acan*
45
46 and *Col2a1* was increased in OA-like explants co-cultured with mMSCs compared with explants
47
48 alone, indicating a chondroinductive effect of mMSCs (Fig. 2A). As femoral head explants are
49
50 made of several tissues (cartilage, bone and bone marrow), we evaluated the effect of mMSCs
51
52 specifically on OA-like chondrocytes (experimental strategy in Fig. 1F). Co-culture with mMSCs
53
54 did not significantly change the expression of anabolic, catabolic and inflammatory factors in
55
56
57
58
59
60
61
62
63
64
65

1
2
3
4 OA-like chondrocytes. Conversely, addition of mMSC-CM increased *Acan* expression, compared
5
6 with OA-like chondrocytes alone, but without reaching the levels of chondrocytes not exposed
7
8 to IL1 β . The expression of type IIB collagen and of catabolic and inflammatory mediators was
9
10 not modified by addition of mMSC-CM (Fig. 2B-C). Finally, we evaluated whether co-culture with
11
12 hMSCs influenced the phenotype of murine OA-like chondrocytes and found no significant
13
14 change, except for a decrease of iNOS expression (Fig. 2D).
15
16
17
18
19
20
21

22 **TGF β 3-primed murine and human MSCs reverse the deregulation of cartilage markers in**
23
24 **OA-like chondrocytes.** As the TGF β pathway has regulatory functions in cartilage homeostasis
25
26 (REF) and TGFBI downregulation in OA MSCs impairs their functional properties (REF), we tested
27
28 whether TGFBI upregulation in MSCs modified their effect on OA-like chondrocytes. We first
29
30 showed that priming with TGF β 3 upregulated *TGFBI* transcription in mMSCs and hMSCs by 2-
31
32 and 3-fold, respectively (Fig. 3A-B) and increased TGFBI secretion by 3.5-fold in hMSCs (Fig. 3B,
33
34 right panel). Moreover, incubation of OA-like mouse chondrocytes with TGF β 3-primed mMSC-
35
36 CM significantly upregulated the expression of chondrocyte anabolic markers, but did not
37
38 change the expression of catabolic and inflammatory factors (Fig. 3C). Co-culture of OA-like
39
40 chondrocytes with TGF β 3-primed mMSCs led to upregulation of anabolic markers and
41
42 downregulation of catabolic markers, but did not significantly modulate inflammation-
43
44 associated markers (Fig. 3D). Conversely, co-culture with TGF β 3-primed hMSCs significantly
45
46 reversed the deregulated expression of all tested markers, including inflammatory mediators
47
48 (Fig. 3E). Altogether, these results indicated that mMSC pro-anabolic function is regulated by
49
50
51
52
53
54
55
56
57
58
59
60
61
62
63
64
65

1
2
3
4 TGFβ3-priming. However, their anti-catabolic role requires both TGFβ3-priming and co-culture,
5
6
7 indicating the importance of the crosstalk with OA-like chondrocytes.
8
9

10
11 **TGFBI silencing in murine MSCs partly impairs their chondroinductive effect on OA-like**
12 **chondrocytes.** We then investigated the effect of TGFBI downregulation in mMSCs after
13
14
15 transfection with a siTGFBI that reduced by 33% *Tgfb1* mRNA level compared with siCT (Fig. 4A).
16
17
18 This decrease was sufficient to inhibit mMSC chondroinductive effect, as shown by the absence
19
20
21 of *Acan* and *Col2a1* upregulation in OA-like chondrocytes co-cultured with siTGFBI-transfected
22
23
24 mMSCs compared with siCT-mMSCs (Fig. 4A). Similarly, *Acan* upregulation was slightly but
25
26
27 significantly lower in OA-like chondrocytes co-cultured with TGFβ3-primed siTGFBI-mMSCs than
28
29
30 with TGFβ3-primed siCT-mMSCs (Fig. 4B). Finally, siTGFBI transfection in hMSCs reduced *TGFBI*
31
32
33 expression by 48% (Fig. 4C). However, TGFBI downregulation did not modify the expression of
34
35
36 *Acan* and *Col2a1* in OA-like chondrocytes co-cultured with TGFβ3-primed siTGFBI hMSCs.
37
38
39

40 **TGFBI silencing impairs the therapeutic function of human MSCs in CIOA mice.** Then, we
41
42
43 evaluated *in vivo* the effect of IA injection of siCT- or siTGFBI-transfected hMSCs (TGFBI
44
45
46 expression reduced by 70%) in CIOA mice [29]. Histological analysis showed that the OA score
47
48
49 was lower, although not significantly, in CIOA mice treated with siCT-hMSCs compared with
50
51
52 untreated mice (Fig. 5A-B). Conversely, the score was significantly higher in mice treated with
53
54
55 siTGFBI-hMSCs compared with mice treated with siCT-hMSCs and untreated controls.
56
57
58 Histomorphometric analysis of cartilage by CLSM confirmed that cartilage degradation was
59
60
61 more important, and cartilage thickness was lower in CIOA mice treated with siTGFBI-hMSCs
62
63
64
65

1
2
3
4 compared with siCT-hMSCs (Fig. 5C-D). Accordingly, micro-CT analysis showed that sub-chondral
5
6 bone parameters in CIOA mice treated with siCT-hMSCs were similar to those of healthy mice.
7
8 Conversely, CIOA mice that received siTGFBI-hMSCs were not protected from bone degradation
9
10 (Fig. 5E-F). Finally, injection of siCT-hMSCs, but not of siTGFBI-hMSCs partly inhibited
11
12 calcification of the lateral and medial menisci and ligaments in CIOA mice (Fig. 5G-H). Overall,
13
14 these findings indicated that TGFBI produced by hMSCs contributes to their therapeutic effect in
15
16 CIOA mice.
17
18
19
20
21
22
23
24

25 **TGFBI is conveyed within MSC-derived extracellular vesicles.** To understand TGFBI
26
27 mechanism of action, we assessed its effect on chondrocyte functions. Addition of rhTGFBI
28
29 enhanced the proliferation of murine chondrocytes, while culture in rhTGFBI-coated dishes
30
31 reduced chondrocyte adhesion (Fig. 6A-B). Moreover, splenocyte proliferation was slightly, but
32
33 significantly reduced by siTGFBI-transfected hMSCs, suggesting decreased immunosuppressive
34
35 properties upon TGFBI silencing (Fig. 6C). Then, we asked whether TGFBI could be conveyed by
36
37 MSC-EVs that have been shown to have immunomodulatory effects in an arthritis model [23]
38
39 and to transfer MSC-secreted factors between cells [4]. Using an already validated protocol for
40
41 mMSC-EVs, we isolated and characterized total EVs from hMSCs [23]. The quantity of hMSC-EVs
42
43 was 8×10^8 particles/ μg total proteins/ 10^6 hMSCs, and their size ranged from 80 to 400 nm (Fig.
44
45 6D). They expressed surface markers of hMSCs (CD44, CD73, and CD90) and of exosomes (CD63
46
47 and CD81) (Fig. 6E). We detected easily quantifiable amounts of TGFBI protein in hMSC-EVs,
48
49 although the amounts were lower than in hMSCs (Fig. 6F). We also detected *TGFBI* mRNA in
50
51 hMSC-EVs and in small-size and large-size mMSC-EVs (Fig. 6G-H).
52
53
54
55
56
57
58
59
60
61
62
63
64
65

1
2
3
4
5
6
7 **DISCUSSION**
8
9

10
11
12 This is the first evidence that TGFBI produced by hMSCs exerts a pro-anabolic function on
13 chondrocytes and a therapeutic role in OA by preventing cartilage and bone degradation, while
14 inhibiting soft tissue calcification.
15
16
17
18
19

20 Using two *in vitro* models that mimic the cartilage degradation and chondrocyte
21 deregulation observed in OA, we revealed TGFBI expression deregulation in OA-like cartilage.
22 Specifically, TGFBI was upregulated in OA-like femoral head explants, while it was
23 downregulated in OA-like chondrocytes. A possible explanation for this discrepancy might be
24 related to the developmental stage of the analysed tissues. In femoral head explants from 2-3-
25 week-old mice, TGFBI expression is typical of the adult age, and increases in OA-like conditions
26 as observed in epiphyses of CIOA-induced adult mice. This upregulation might be related to a
27 regulatory loop to inhibit cartilage mineralization that occurs during OA. Indeed, it was
28 previously shown that TGFBI inhibits osteogenesis and mineralization of cultured chondrocytes
29 [30-32]. On the other hand, in immature chondrocytes isolated from femoral and tibial
30 epiphyses of 3-day-old mice, TGFBI was downregulated in OA-like conditions. In mouse embryos
31 (E16.5 to E18.5), TGFBI is expressed in proliferating chondrocytes and in primary endochondral
32 ossification centres during joint cartilage formation, where it may interact with cells and
33 extracellular matrix molecules, thus playing a role in tissue morphogenesis [33-35]. In 3-day-old
34 mice, cartilage is predominantly pre-hypertrophic and hypertrophic, consistent with high TGFBI
35 expression, as observed during embryogenesis. We previously reported that TGFBI is required at
36
37
38
39
40
41
42
43
44
45
46
47
48
49
50
51
52
53
54
55
56
57
58
59
60
61
62
63
64
65

1
2
3
4 the early stages of chondrogenic differentiation of MSCs, and is then downregulated in
5
6 mineralized hypertrophic chondrocytes [21]. The present study brings evidence that besides
7
8 promoting endochondral ossification and inhibiting mineralization during *in vitro* differentiation
9
10 of mature osteoblasts or chondrocytes, TGFBI deregulation in joint tissues might contribute to
11
12
13
14 OA.

15
16
17 TGFBI is a paralogue of periostin (*POSTN*), the only other member of the TGFBI family. The
18
19 two genes have a similar domain structure, although *TGFBI* is shorter and lacks the C-terminal
20
21 domain that is subjected to alternative splicing in *POSTN* [36, 37]. Both genes have important
22
23 overlapping functions in cell adhesion, migration, proliferation, and apoptosis. In cancer, they
24
25 display dual roles, acting as tumour suppressors or promoters, depending on the tumour
26
27 environment. *POSTN* levels in serum and synovial fluid are associated with OA incidence and
28
29 progression [38, 39], and its expression is higher in mouse and human bone and cartilage [40,
30
31 41]. Importantly, the higher chondroprotective effect in OA mice of FRA-1-overexpressing
32
33 adipose-derived stromal cells compared with wild type cells has been associated with increased
34
35 *POSTN* expression [42]. We recently reported TGFBI upregulation in bone and cartilage from
36
37 patients and mice with OA [21]. Based on the similarity of functions and expression in OA, all
38
39 these data suggest a possible common regulation of *POSTN* and TGFBI in OA and identify these
40
41 two molecules as important players in joint homeostasis. In agreement, the present study
42
43 demonstrated the lower *in vivo* therapeutic efficiency of siTGFBI-hMSCs that mimic the lower
44
45 TGFBI expression of hMSCs from patients with OA. Interestingly, siTGFBI-hMSCs could not
46
47 reduce osteophyte calcification in CIOA mice (data not shown), further supporting a probable
48
49 inhibitory role of TGFBI on mineralization *in vivo*. TGF β pathway deregulation in MSCs was
50
51
52
53
54
55
56
57
58
59
60
61
62
63
64
65

1
2
3
4 previously associated with OA onset and/or maintenance [20]. Here, we present further
5
6 evidence that TGFBI deregulation in OA MSCs impairs their therapeutic chondroprotective
7
8 function and might affect their physiologic role in cartilage and bone homeostasis.
9

10
11 We provided evidence that EVs released by mMSCs and hMSCs contain both TGFBI mRNA
12
13 and protein, underlining a plausible common mechanism of action. Usually, EVs act on target
14
15 cells after their internalization mediated by fusion of their membrane with the cell plasma
16
17 membrane or after uptake. After uptake, EVs are addressed to the canonical endosomal
18
19 pathway and can be targeted to lysosomes and degraded, or can discharge their cargo in the
20
21 cytosol by fusion with the endosomal membrane [43]. A possible transfer of EVs to the plasma
22
23 membrane for release might also occur. In our conditions, we could not detect the presence of
24
25 human *TGFBI* mRNA in murine chondrocytes after 1 day of co-culture with hMSCs (data not
26
27 shown), possibly because after uptake, the amount of *TGFBI* mRNA released in chondrocytes
28
29 might have been too low to be detected, or rapidly degraded or translated into proteins.
30
31 Further investigations are needed to determine the fate of EV cargoes in chondrocytes or
32
33 synovial cells in the joint. Nevertheless, we previously demonstrated that IA injection of small-
34
35 size and large size mMSC-EVs can protect mice from developing CIOA to a similar extent as
36
37 mMSCs, suggesting that TGFBI mRNA and protein contained in EVs might play an important role
38
39 [27]. The relative contribution of soluble TGFBI and EV-contained TGFBI needs to be
40
41 investigated.
42
43
44
45
46
47
48
49
50
51

52
53 One of the main roles of TGFBI is to mediate cell adhesion and migration by acting as a
54
55 linker that connects various matrix molecules and favours cell-collagen interactions. This has
56
57 been shown mainly in tumour cells where TGFBI can act either as tumour promoter by
58
59
60
61
62
63
64
65

1
2
3
4 increasing cancer cell invasiveness, or as a tumour suppressor by inhibiting cell adhesion leading
5
6 to inhibition of cell proliferation and migration [44]. TGFBI also increases cell survival and
7
8 proliferation during gastrointestinal tract tumorigenesis via activation of the FAK/AKT signalling
9
10 pathway [45]. Moreover, TGFBI expression is a predictor of survival in patients with lung
11
12 squamous cell carcinoma [46]. However, its physiological role is still unclear. Here, we
13
14 demonstrated that TGFBI decreases chondrocyte adhesion and increases their proliferation.
15
16 Therefore, TGFBI secreted by MSCs might mediate its therapeutic effect in joint tissues via a
17
18 pro-survival and pro-anabolic role on chondrocytes.
19
20
21
22
23
24

25 TGFBI could also have an anti-inflammatory effect through its negative regulation of Toll
26
27 like receptor-induced inflammation. For instance, TGFBI expression was increased in peripheral
28
29 blood mononuclear cells in a model of lipopolysaccharide-induced endotoxin tolerance,
30
31 resulting in lower activation of inflammatory actors, such as nuclear factor- κ B, TNF- α and nitric
32
33 oxide [47]. Moreover, a significant correlation has been observed between three single
34
35 nucleotide polymorphisms in the *TGFBI* gene and type 1 diabetes, and TGFBI expression is lower
36
37 in pancreatic islets from diabetic subjects. Interestingly, TGFBI can inhibit T-cell activation
38
39 markers (CD44 and CD69) and the production of cytotoxic molecules, such as granzyme B and
40
41 interferon- γ [48]. In addition, TGFBI-treated diabetogenic T cells cannot induce type 1 diabetes
42
43 upon transfer in wild type mice, suggesting that TGFBI expression in pancreatic islets might
44
45 contribute as a protective shield against cytotoxic T-cell attack. Our data indicated that TGFBI
46
47 plays a role in MSC anti-inflammatory function and contributes to T lymphocyte proliferation
48
49 inhibition. Therefore, the hypothesis that TGFBI released by hMSCs might exert an anti-
50
51 inflammatory function in OA should be investigated *in vivo*.
52
53
54
55
56
57
58
59
60
61
62
63
64
65

1
2
3
4
5
6
7
8
9
10
11
12
13
14
15
16
17
18
19
20
21
22
23
24
25
26
27
28
29
30
31
32
33
34
35
36
37
38
39
40
41
42
43
44
45
46
47
48
49
50
51
52
53
54
55
56
57
58
59
60
61
62
63
64
65

All experimental data required to reproduce the findings from this study will be made available to interested investigators.

AUTHOR CONTRIBUTIONS

DN, CJ designed the experiments. Experimental work was performed by MR, MM, KT, PR, DN. MR, MM, KT, PR, CJ, DN analysed the data and prepared the manuscript. All authors have contributed to writing or revising the manuscript and final approval.

REFERENCES

- [1] R. Hass, C. Kasper, S. Bohm, R. Jacobs, Different populations and sources of human mesenchymal stem cells (MSC): A comparison of adult and neonatal tissue-derived MSC, *Cell Commun Signal* 9 (2011) 12.
- [2] M. Dominici, K. Le Blanc, I. Mueller, I. Slaper-Cortenbach, F. Marini, D. Krause, R. Deans, A. Keating, D. Prockop, E. Horwitz, Minimal criteria for defining multipotent mesenchymal stromal cells. The International Society for Cellular Therapy position statement, *Cytotherapy* 8(4) (2006) 315-7.
- [3] J. Galipeau, M. Krampera, J. Barrett, F. Dazzi, R.J. Deans, J. DeBruijn, M. Dominici, W.E. Fibbe, A.P. Gee, J.M. Gimble, P. Hematti, M.B. Koh, K. LeBlanc, I. Martin, I.K. McNiece, M. Mendicino, S. Oh, L. Ortiz, D.G. Phinney, V. Planat, Y. Shi, D.F. Stroncek, S. Viswanathan, D.J. Weiss, L. Sensebe, International Society for Cellular Therapy perspective on immune functional assays for mesenchymal stromal cells as potency release criterion for advanced phase clinical trials, *Cytotherapy* 18(2) (2016) 151-9.
- [4] S. Cosenza, M. Ruiz, M. Maumus, C. Jorgensen, D. Noel, Pathogenic or Therapeutic Extracellular Vesicles in Rheumatic Diseases: Role of Mesenchymal Stem Cell-Derived Vesicles, *Int J Mol Sci* 18(4) (2017).
- [5] C. Bouffi, C. Bony, G. Courties, C. Jorgensen, D. Noel, IL-6-dependent PGE2 secretion by mesenchymal stem cells inhibits local inflammation in experimental arthritis, *PLoS One* 5(12) (2010) e14247.
- [6] P. Luz-Crawford, F. Djouad, K. Toupet, C. Bony, M. Franquesa, M.J. Hoogduijn, C. Jorgensen, D. Noel, Mesenchymal Stem Cell-Derived Interleukin 1 Receptor Antagonist Promotes Macrophage Polarization and Inhibits B Cell Differentiation, *Stem Cells* 34(2) (2016) 483-92.
- [7] P. Luz-Crawford, G. Tejedor, A.L. Mausset-Bonnefont, E. Beaulieu, E.F. Morand, C. Jorgensen, D. Noel, F. Djouad, Gilz governs the therapeutic potential of mesenchymal stem cells by inducing a switch from pathogenic to regulatory Th17 cells, *Arthritis Rheumatol* 67(6) (2015) 1514-24.
- [8] M. Maumus, C. Manferdini, K. Toupet, P. Chuchana, L. Casteilla, M. Gachet, C. Jorgensen, G. Lisignoli, D. Noel, Thrombospondin-1 Partly Mediates the Cartilage Protective Effect of Adipose-Derived Mesenchymal Stem Cells in Osteoarthritis, *Front Immunol* 8 (2017) 1638.
- [9] A. Mobasheri, M. Batt, An update on the pathophysiology of osteoarthritis, *Ann Phys Rehabil Med* 59(5-6) (2016) 333-339.
- [10] F. Berenbaum, T.M. Griffin, R. Liu-Bryan, Review: Metabolic Regulation of Inflammation in Osteoarthritis, *Arthritis Rheumatol* 69(1) (2017) 9-21.
- [11] M.B. Goldring, F. Berenbaum, Emerging targets in osteoarthritis therapy, *Curr Opin Pharmacol* 22 (2015) 51-63.
- [12] G. Desando, C. Cavallo, F. Sartoni, L. Martini, A. Parrilli, F. Veronesi, M. Fini, R. Giardino, A. Facchini, B. Grigolo, Intra-articular delivery of adipose derived stromal cells attenuates osteoarthritis progression in an experimental rabbit model, *Arthritis Res Ther* 15(1) (2013) R22.
- [13] J.M. Murphy, D.J. Fink, E.B. Hunziker, F.P. Barry, Stem cell therapy in a caprine model of osteoarthritis, *Arthritis Rheum* 48(12) (2003) 3464-74.
- [14] M. Ter Huurne, R. Schelbergen, R. Blattes, A. Blom, W. de Munter, L.C. Grevers, J. Jeanson, D. Noel, L. Casteilla, C. Jorgensen, W. van den Berg, P.L. van Lent, Antiinflammatory and chondroprotective effects of intraarticular injection of adipose-derived stem cells in experimental osteoarthritis, *Arthritis Rheum* 64(11) (2012) 3604-13.
- [15] M. Ruiz, S. Cosenza, M. Maumus, C. Jorgensen, D. Noel, Therapeutic application of mesenchymal stem cells in osteoarthritis, *Expert Opin Biol Ther* 16(1) (2015) 33-42.

- 1
2
3
4 [16] M.M. Schimke, S. Marozin, G. Lepperdinger, Patient-Specific Age: The Other Side of the Coin in
5 Advanced Mesenchymal Stem Cell Therapy, *Front Physiol* 6 (2015) 362.
- 6 [17] N. Baker, L.B. Boyette, R.S. Tuan, Characterization of bone marrow-derived mesenchymal stem cells
7 in aging, *Bone* 70 (2015) 37-47.
- 8 [18] G. Zhai, J. Dore, P. Rahman, TGF-beta signal transduction pathways and osteoarthritis, *Rheumatol*
9 *Int* 35(8) (2015) 1283-92.
- 10 [19] P.M. van der Kraan, The changing role of TGFbeta in healthy, ageing and osteoarthritic joints, *Nat*
11 *Rev Rheumatol* 13(3) (2017) 155-163.
- 12 [20] G. Zhen, C. Wen, X. Jia, Y. Li, J.L. Crane, S.C. Mears, F.B. Askin, F.J. Frassica, W. Chang, J. Yao, J.A.
13 Carrino, A. Cosgarea, D. Artemov, Q. Chen, Z. Zhao, X. Zhou, L. Riley, P. Sponseller, M. Wan, W.W. Lu, X.
14 Cao, Inhibition of TGF-beta signaling in mesenchymal stem cells of subchondral bone attenuates
15 osteoarthritis, *Nat Med* 19(6) (2013) 704-12.
- 16 [21] M. Ruiz, M. Maumus, G. Fonteneau, Y.M. Pers, R. Ferreira, L. Dagneaux, C. Delfour, X. Houard, F.
17 Berenbaum, F. Rannou, C. Jorgensen, D. Noel, TGFbeta1 is involved in the chondrogenic differentiation of
18 mesenchymal stem cells and is dysregulated in osteoarthritis, *Osteoarthritis Cartilage* 27(3) (2019) 493-
19 503.
- 20 [22] A.T. Maria, K. Toupet, M. Maumus, G. Fonteneau, A. Le Quellec, C. Jorgensen, P. Guilpain, D. Noel,
21 Human adipose mesenchymal stem cells as potent anti-fibrosis therapy for systemic sclerosis, *J*
22 *Autoimmun* 70 (2016) 31-9.
- 23 [23] S. Cosenza, K. Toupet, M. Maumus, P. Luz-Crawford, O. Blanc-Brude, C. Jorgensen, D. Noel,
24 Mesenchymal stem cells-derived exosomes are more immunosuppressive than microparticles in
25 inflammatory arthritis, *Theranostics* 8(5) (2018) 1399-1410.
- 26 [24] H. Stanton, S.B. Golub, F.M. Rogerson, K. Last, C.B. Little, A.J. Fosang, Investigating ADAMTS-
27 mediated aggrecanolysis in mouse cartilage, *Nat Protoc* 6(3) (2011) 388-404.
- 28 [25] M. Gosset, F. Berenbaum, S. Thirion, C. Jacques, Primary culture and phenotyping of murine
29 chondrocytes, *Nat Protoc* 3(8) (2008) 1253-60.
- 30 [26] S. Domergue, C. Bony, M. Maumus, K. Toupet, E. Frouin, V. Rigau, M.C. Vozenin, G. Magalon, C.
31 Jorgensen, D. Noel, Comparison between Stromal Vascular Fraction and Adipose Mesenchymal Stem
32 Cells in Remodeling Hypertrophic Scars, *PLoS One* 11(5) (2016) e0156161.
- 33 [27] S. Cosenza, M. Ruiz, K. Toupet, C. Jorgensen, D. Noel, Mesenchymal stem cells derived exosomes
34 and microparticles protect cartilage and bone from degradation in osteoarthritis, *Sci Rep* 7(1) (2017)
35 16214.
- 36 [28] M. Ruiz, M. Maumus, G. Fonteneau, Y.M. Pers, R. Ferreira, L. Dagneaux, C. Delfour, X. Houard, F.
37 Berenbaum, F. Rannou, C. Jorgensen, D. Noel, TGFbeta1 is involved in the chondrogenic differentiation of
38 mesenchymal stem cells and is dysregulated in osteoarthritis, *Osteoarthritis Cartilage* (2018).
- 39 [29] K. Toupet, M. Maumus, P. Luz-Crawford, E. Lombardo, J. Lopez-Belmonte, P. van Lent, M.I. Garin, W.
40 van den Berg, W. Dalemans, C. Jorgensen, D. Noel, Survival and biodistribution of xenogenic adipose
41 mesenchymal stem cells is not affected by the degree of inflammation in arthritis, *PLoS One* 10(1) (2015)
42 e0114962.
- 43 [30] M.J. Lee, S.C. Heo, S.H. Shin, Y.W. Kwon, E.K. Do, D.S. Suh, M.S. Yoon, J.H. Kim, Oncostatin M
44 promotes mesenchymal stem cell-stimulated tumor growth through a paracrine mechanism involving
45 periostin and TGFBI, *Int J Biochem Cell Biol* 45(8) (2013) 1869-77.
- 46 [31] J. Ren, P. Jin, M. Sabatino, A. Balakumaran, J. Feng, S.A. Kuznetsov, H.G. Klein, P.G. Robey, D.F.
47 Stroncek, Global transcriptome analysis of human bone marrow stromal cells (BMSC) reveals
48 proliferative, mobile and interactive cells that produce abundant extracellular matrix proteins, some of
49 which may affect BMSC potency, *Cytotherapy* 13(6) (2011) 661-74.
- 50
51
52
53
54
55
56
57
58
59
60
61
62
63
64
65

- 1
2
3
4 [32] R. Bhushan, J. Grunhagen, J. Becker, P.N. Robinson, C.E. Ott, P. Knaus, miR-181a promotes
5 osteoblastic differentiation through repression of TGF-beta signaling molecules, *Int J Biochem Cell Biol*
6 45(3) (2013) 696-705.
7
8 [33] J.W. Ferguson, M.F. Mikesch, E.F. Wheeler, R.G. LeBaron, Developmental expression patterns of
9 Beta-ig (betaIG-H3) and its function as a cell adhesion protein, *Mech Dev* 120(8) (2003) 851-64.
10 [34] M.S. Han, J.E. Kim, H.I. Shin, I.S. Kim, Expression patterns of betaig-h3 in chondrocyte differentiation
11 during endochondral ossification, *Exp Mol Med* 40(4) (2008) 453-60.
12 [35] S. Ohno, T. Doi, S. Tsutsumi, Y. Okada, K. Yoneno, Y. Kato, K. Tanne, RGD-CAP ((beta)ig-h3) is
13 expressed in precartilag condensation and in prehypertrophic chondrocytes during cartilage
14 development, *Biochim Biophys Acta* 1572(1) (2002) 114-22.
15 [36] X. Song, L. Cai, Y. Li, J. Zhu, P. Jin, L. Chen, F. Ma, Identification and characterization of transforming
16 growth factor beta induced gene (TGFBIG) from Branchiostoma belcheri: insights into evolution of TGFBIG
17 family, *Genomics* 103(1) (2014) 147-53.
18 [37] D.F. Mosher, M.W. Johansson, M.E. Gillis, D.S. Annis, Periostin and TGF-beta-induced protein: Two
19 peas in a pod?, *Crit Rev Biochem Mol Biol* 50(5) (2015) 427-39.
20 [38] S. Honsawek, V. Wilairatana, W. Udomsinprasert, P. Sinlapavilawan, N. Jirathanathornnukul,
21 Association of plasma and synovial fluid periostin with radiographic knee osteoarthritis: Cross-sectional
22 study, *Joint Bone Spine* 82(5) (2015) 352-5.
23 [39] J.C. Rousseau, E. Sornay-Rendu, C. Bertholon, P. Garnero, R. Chapurlat, Serum periostin is associated
24 with prevalent knee osteoarthritis and disease incidence/progression in women: the OFELY study,
25 *Osteoarthritis Cartilage* 23(10) (2015) 1736-42.
26 [40] C.H. Chou, C.C. Wu, I.W. Song, H.P. Chuang, L.S. Lu, J.H. Chang, S.Y. Kuo, C.H. Lee, J.Y. Wu, Y.T. Chen,
27 V.B. Kraus, M.T. Lee, Genome-wide expression profiles of subchondral bone in osteoarthritis, *Arthritis*
28 *Res Ther* 15(6) (2013) R190.
29 [41] R.F. Loeser, A.L. Olex, M.A. McNulty, C.S. Carlson, M.F. Callahan, C.M. Ferguson, J. Chou, X. Leng, J.S.
30 Fetrow, Microarray analysis reveals age-related differences in gene expression during the development
31 of osteoarthritis in mice, *Arthritis Rheum* 64(3) (2012) 705-17.
32 [42] K. Schwabe, M. Garcia, K. Ubieta, N. Hannemann, B. Herbort, J. Luther, D. Noel, C. Jorgensen, L.
33 Casteilla, J.P. David, M. Stock, M. Herrmann, G. Schett, A. Bozec, Inhibition of Osteoarthritis by Adipose-
34 Derived Stromal Cells Overexpressing Fra-1 in Mice, *Arthritis Rheumatol* 68(1) (2016) 138-51.
35 [43] G. van Niel, G. D'Angelo, G. Raposo, Shedding light on the cell biology of extracellular vesicles, *Nat*
36 *Rev Mol Cell Biol* 19(4) (2018) 213-228.
37 [44] M.P. Ween, M.K. Oehler, C. Ricciardelli, Transforming growth Factor-Beta-Induced Protein
38 (TGFBIG)/(betaig-H3): a matrix protein with dual functions in ovarian cancer, *Int J Mol Sci* 13(8) (2012)
39 10461-77.
40 [45] B. Han, H. Cai, Y. Chen, B. Hu, H. Luo, Y. Wu, J. Wu, The role of TGFBIG (betaig-H3) in gastrointestinal
41 tract tumorigenesis, *Mol Cancer* 14 (2015) 64.
42 [46] M.J. Pajares, J. Agorreta, E. Salvo, C. Behrens, Wistuba, II, L.M. Montuenga, R. Pio, A. Rouzaut, TGFBIG
43 expression is an independent predictor of survival in adjuvant-treated lung squamous cell carcinoma
44 patients, *Br J Cancer* 110(6) (2014) 1545-51.
45 [47] Y. Yang, H. Sun, X. Li, Q. Ding, P. Wei, J. Zhou, Transforming Growth Factor Beta-Induced Is Essential
46 for Endotoxin Tolerance Induced by a Low Dose of Lipopolysaccharide in Human Peripheral Blood
47 Mononuclear Cells, *Iran J Allergy Asthma Immunol* 14(3) (2015) 321-30.
48 [48] M. Patry, R. Teinturier, D. Goehrig, C. Zetu, D. Ripoche, I.S. Kim, P. Bertolino, A. Hennino, betaig-h3
49 Represses T-Cell Activation in Type 1 Diabetes, *Diabetes* 64(12) (2015) 4212-9.
50
51
52
53
54
55
56
57
58
59
60
61
62
63
64
65

Figure legends

Figure 1. Modulation of TGFBI expression in mouse tissues and in *in vitro* OA-like models. A) *Tgfb1* mRNA expression in the indicated tissues from 3-day-old healthy mice. B) *Tgfb1* mRNA expression in the indicated tissues from adult mice. C) *Tgfb1* mRNA expression in epiphyses from adult healthy mice and after OA induction. D) Scheme showing the OA-like model based on incubation of adult femoral head explants with IL1 β . E) RT-qPCR analysis of different chondrocyte markers and TGFBI in control (NT, not treated with IL1 β) and OA-like femoral head explants (IL1 β). Glycosaminoglycan (GAG) quantification in femoral head explants, and GAG release in the culture medium from NT and IL1 β -treated samples after 3 days. F) Scheme explaining the generation of OA-like chondrocytes by incubation with IL1 β . G) RT-qPCR analysis of different chondrocyte and inflammatory markers and of TGFBI in control (NT, not treated with IL1 β) and OA-like chondrocytes (IL1 β). Each dot represents one biological replicate, and results are expressed as the mean \pm SEM. Groups were compared with the Kruskal-Wallis test followed by the Dunn's multiple comparisons test in (A-B), the Mann-Whitney test in (C, E, G), or the Wilcoxon signed-rank test to compare NT and IL1 β -treated samples (dotted line) (E, G). *: $p < 0.05$; **: $p < 0.01$; ***: $p < 0.001$, and ****: $p < 0.0001$.

Figure 2. Effect of mMSCs and hMSCs on chondrocyte gene expression in the *in vitro* OA-like models. A) Glycosaminoglycan (GAG) quantification in the supernatant of OA-like femoral head explants (IL1 β) after 3 days of co-culture or not with mMSCs (left). RT-qPCR analysis of the chondrocyte markers *Col2a1* (middle) and *Acan* (right) in control (NT, not treated with IL1 β)

1
2
3
4 and OA-like femoral head explants (IL1 β) after 3 days of co-culture or not with mMSCs (n=5-10
5
6 biological replicates). B) RT-qPCR analysis of different chondrocyte and inflammatory markers in
7
8 control (NT, not treated with IL1 β) and OA-like chondrocytes (IL1 β) incubated or not with mMSC
9
10 conditioned medium (mMSC-CM). C) RT-qPCR analysis of different chondrocyte and
11
12 inflammatory markers in control (NT) and OA-like chondrocytes (IL1 β) co-cultured or not with
13
14 mMSCs. D) RT-qPCR analysis of different chondrocyte and inflammatory markers in control (NT)
15
16 and OA-like chondrocytes (IL1 β) co-cultured or not with hMSCs. Each dot represents one
17
18 biological replicate, and results are expressed as the mean \pm SEM. Two groups were compared
19
20 with the Mann-Whitney test (A), and samples were compared to OA-like chondrocytes (IL1 β ; set
21
22 to 1) with the Wilcoxon signed-rank test (dotted line) (B-D). *: p<0.05; **: p<0.01; ***: p<0.001,
23
24 and ****: p<0.0001.
25
26
27
28
29
30
31
32
33
34

35 Figure 3. Effect of TGF β 3-primed mMSCs and hMSCs on chondrocyte gene expression in *in vitro*
36
37 OA-like models. A) RT-qPCR analysis of *Tgfb1* in mMSCs primed (TGF β 3) or not (NT) with TGF β 3
38
39 (n=17/group). B) RT-qPCR analysis of *TGFBI* (left panel; n=11 biological replicates) and
40
41 quantification of TGFBI in the supernatant (right panel, n=4 biological replicates) of control (NT)
42
43 and TGF β 3-primed hMSCs. C-D) RT-qPCR analysis of chondrocyte and inflammatory markers in
44
45 control (NT, not treated with IL1 β) and OA-like chondrocytes (IL1 β) incubated or not with
46
47 conditioned medium from TGF β 3-primed mMSCs (mMSC-CM*) (C), or co-cultured or not with
48
49 TGF β 3-primed mMSCs (mMSC*) (D). E) RT-qPCR analysis of chondrocyte and inflammatory
50
51 markers in control (NT) and OA-like chondrocytes (IL1 β) co-cultured or not with TGF β 3-primed
52
53 hMSCs (hMSC*). Each dot represents one biological replicate, and results are expressed as the
54
55
56
57
58
59
60
61
62
63
64
65

1
2
3
4 mean \pm SEM. The Mann-Whitney test was used to compare two groups (A), and the Wilcoxon
5
6 signed-rank test to compare samples to IL1 β -treated chondrocytes (set to 1; dotted line) (C-E).

7
8
9 *: p<0.05; **: p<0.01; ***: p<0.001 or ****: p<0.0001.

10
11
12
13
14 Figure 4. Effect of TGFBI silencing in mMSCs and hMSCs on co-cultured OA-like chondrocytes. A)
15
16 RT-qPCR analysis of *Tgfbi* in mMSCs transfected with control (siCT) or anti-TGFBI siRNAs (siTBI)
17
18 and of chondrocyte markers in control (NT, not treated with IL1 β) and OA-like chondrocytes
19
20 (IL1 β) co-cultured or not with siCT- or siTBI-transfected mMSCs (n=8 biological replicates). B) RT-
21
22 qPCR analysis of *Tgfbi* in siCT- and siTBI transfected mMSCs and of chondrocyte genes in control
23
24 (NT) and OA-like chondrocytes (IL1 β) co-cultured or not with siCT- or siTBI-transfected TGF β 3-
25
26 primed mMSCs (mMSCs*; n=12 biological replicates). C) RT-qPCR analysis of *TGFBI* in siCT- and
27
28 siTBI-transfected hMSCs and of chondrocyte genes in control (NT) and OA-like chondrocytes
29
30 (IL1 β) co-cultured or not with siCT- or siTBI-transfected TGF β 3-primed hMSCs (hMSCs*; n=8
31
32 biological replicates). Results are expressed as the mean \pm SEM. The Wilcoxon signed-rank test
33
34 was used to compare OA-like chondrocytes (IL1 β) in different conditions to OA-like
35
36 chondrocytes co-cultured with siCT-mMSCs or hMSCs (set to 1; dotted line). *: p<0.05; **:
37
38 p<0.01.

39
40
41
42
43
44
45
46
47
48
49
50
51 Figure 5. Effect of siTGFBI-hMSCs in the collagenase-induced osteoarthritic (CIOA) murine
52
53 model. A) Histological images of healthy (H) mice and CIOA mice not treated (NT) or treated
54
55 with hMSCs transfected with control (siCT) or anti-TGFBI (siTBI) mRNAs. B) OA score of
56
57 histological sections of knee joints of the mice described in A. C) Histomorphometric analysis of
58
59
60
61
62
63
64
65

1
2
3
4 3D images of cartilage by CLSM. D) Representative 3D reconstructed images of medial tibial
5
6
7 cartilage after CLSM analysis; on the left, colour code for cartilage thickness. E) Representative
8
9
10 3D reconstructed images of the sub-chondral bone surface in tibias after micro-CT analysis. F)
11
12 Histomorphometric analysis of 3D images of sub-chondral bone: thickness and bone
13
14 surface/bone volume (BS/BV) parameters (n=15/group). G) Histomorphometric analysis
15
16 (volume and surface) of mineralized tissues in joints. H) Representative 3D reconstructed
17
18 images of mouse knee joints after micro-CT analysis showing mineralized menisci and external
19
20 ligaments. Results are expressed as the mean \pm SEM; *: p<0.05; ****: p<0.0001 (Mann-Whitney
21
22 test; n=23 mice/group from 2 independent experiments).
23
24
25
26
27
28
29

30 Figure 6. Functional effect of TGFBI. A) Proliferation of chondrocytes on plates coated with
31
32 recombinant hTGFBI, expressed as fold change compared with cells cultured on plates coated
33
34 with PBS (NT). B) Adhesion of chondrocytes on plates coated with PBS (NT) or recombinant
35
36 hTGFBI, expressed as the cell number fold-change relative to NT at the indicated time points
37
38 after seeding normalized (n=9 biological replicates). C) Proliferation of concanavalin A-activated
39
40 mouse splenocytes co-cultured or not with hMSCs transfected with control (siCT) or anti-siTGFBI
41
42 siRNAs at two ratios (1:10 or 1:20, hMSCs:splenocytes) (n=7 biological replicates). D) Number
43
44 and median size of extracellular vesicles from hMSCs (hMSC-EVs) by nano-particle tracking
45
46 analysis. E) Representative histograms of hMSC-EV surface markers by flow cytometry. F) TGFBI
47
48 protein expression in hMSC-EVs and in hMSCs normalized to the total protein amount. G)
49
50 Expression of *TGFBI* mRNA in hMSCs and hMSC-EVs as expressed as Ct value. H) Expression of
51
52
53
54
55
56
57
58
59
60
61
62
63
64
65

1
2
3
4
5
6
7
8
9
10
11
12
13
14
15
16
17
18
19
20
21
22
23
24
25
26
27
28
29
30
31
32
33
34
35
36
37
38
39
40
41
42
43
44
45
46
47
48
49
50
51
52
53
54
55
56
57
58
59
60
61
62
63
64
65

mMSC-IsEVs (large-size EVs), expressed as Ct value. Each dot represents a biological replicate and results are expressed as the mean \pm SEM. *: $p < 0.05$; ****: $p < 0.0001$ (Wilcoxon signed-rank test in (A) and Mann-Whitney test in (B-C)).

Table 1: List of primer sequences for RT-qPCR analysis

Gene	Sequence forward	Sequence reverse
mADAMTS5	CTGCCTTCAAGGCAAATGTGTGG	CAATGGCGGTAGGCAAAGTGC
mAGG	GCGAGTCCAAGTCTTCAAGC	GAAGTAGCAGGGGATGGTGA
mCOL2B	CTGGTGCTGCTGACGCT	GCCCTAATTTTCGGGCAT
mCOX2	GCATTCTTTGCCAGCACTT	AGACCAGGCACCAGACCAAAGA
mIL6	TGGGACTGATGCTGGTGACA	TTCCACGATTTCCAGAGAACA
mINOS	CCTTGTTCAAGCTACGCCTTC	GCTTGTCAACCACCAGCAGTA
mMCP1	TGCAGGTCCCTGTCATGCTT	TCCTTCTTGGGGTCAGCACA
mMMP13	TCTGGATCACTCCAAGGACC	ATCAGGAAGCATGAAATGGC
mTGFB1	ACCATCAACGGGAAGGCTGTCA	AGCCAGCTCAAGCAGTGTCTTG
mTNFalpha	AGCCCACGTCGTAGCAAACCA	TGTCTTTGAGATCCATGCCGTTGGC
hTGFB1	GGACATGCTCACTATCAACGGG	CTGTGGACACATCAGACTCTGC

Figure 1
[Click here to download high resolution image](#)

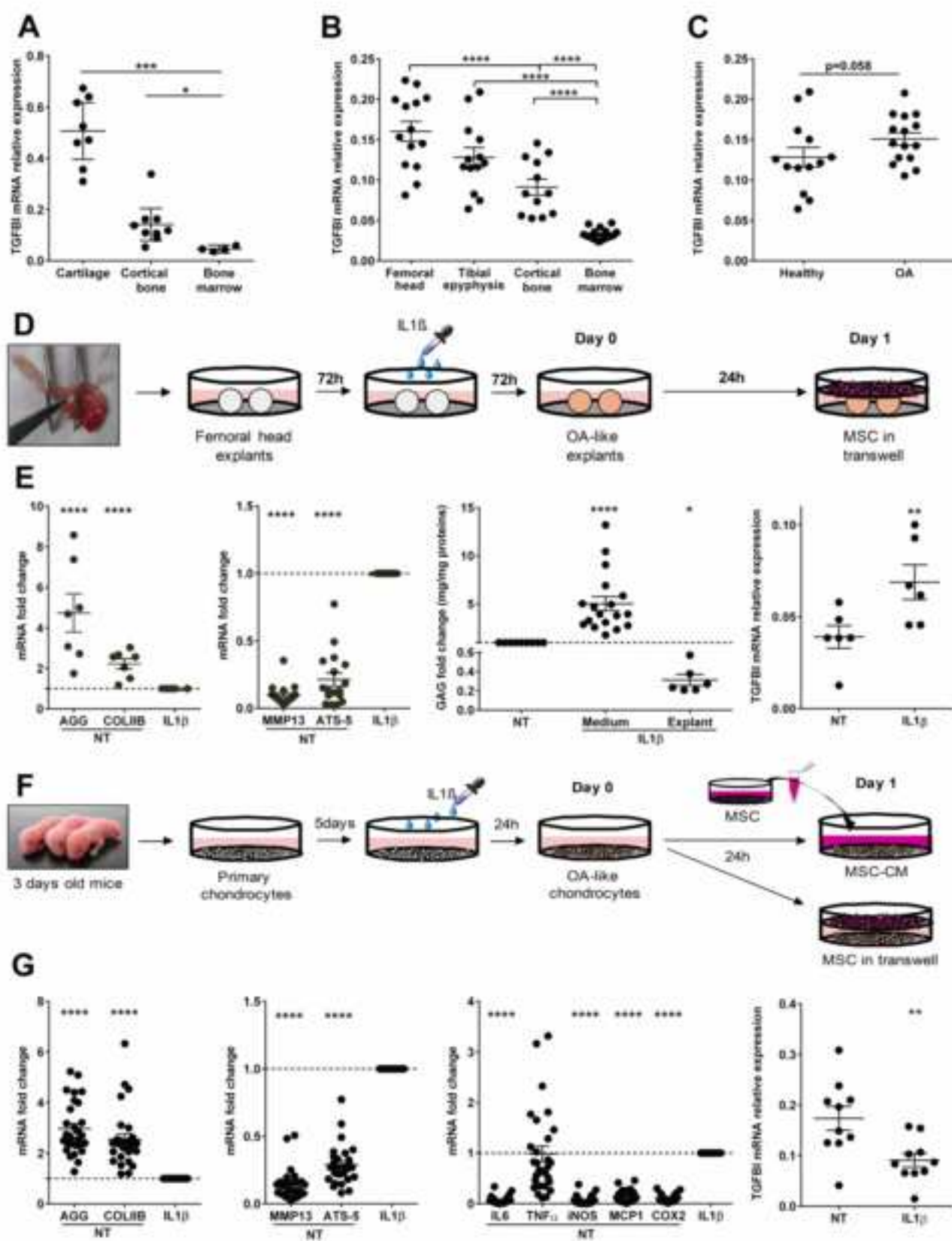


Figure 2

[Click here to download high resolution image](#)

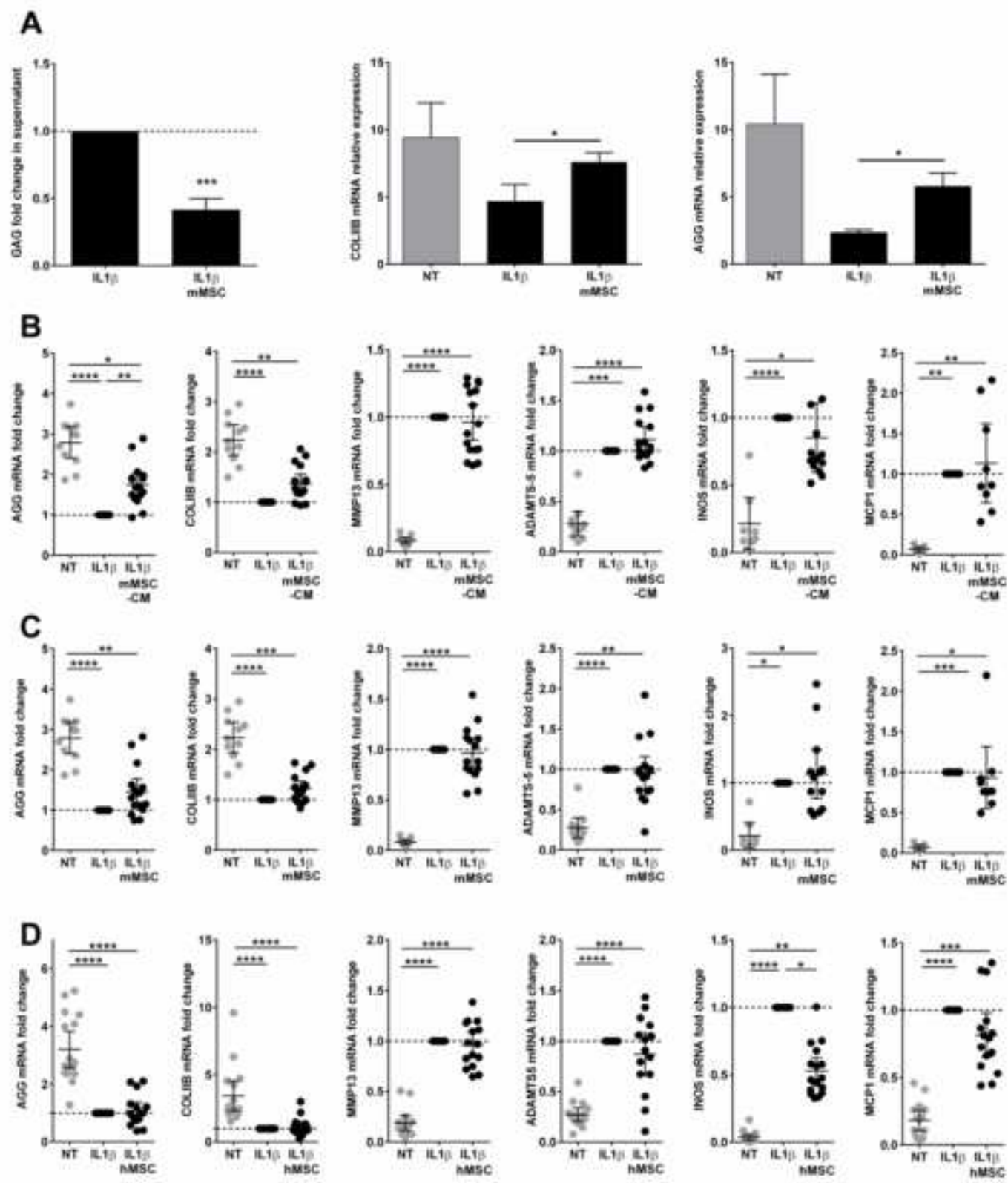


Figure 3

[Click here to download high resolution image](#)

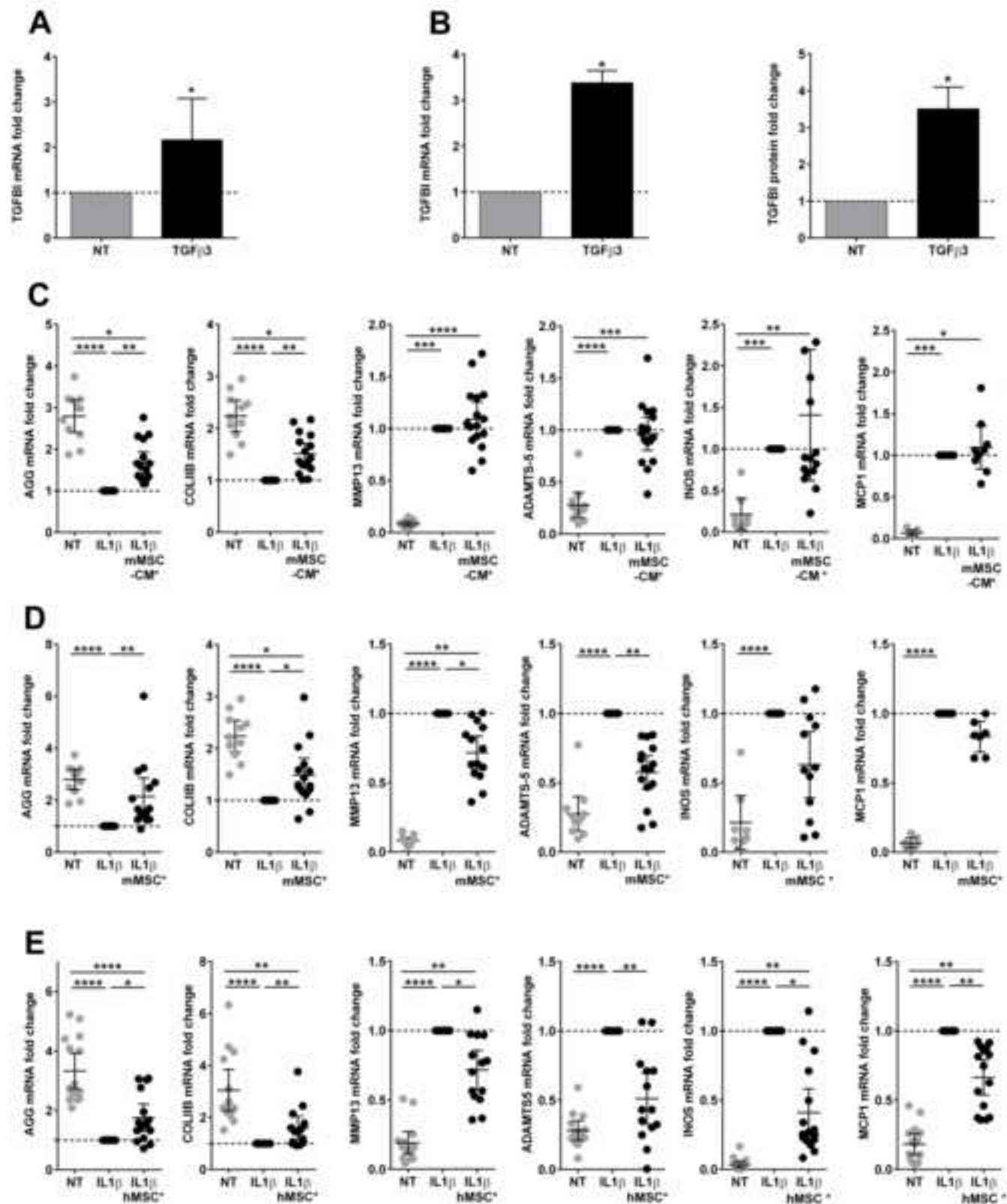
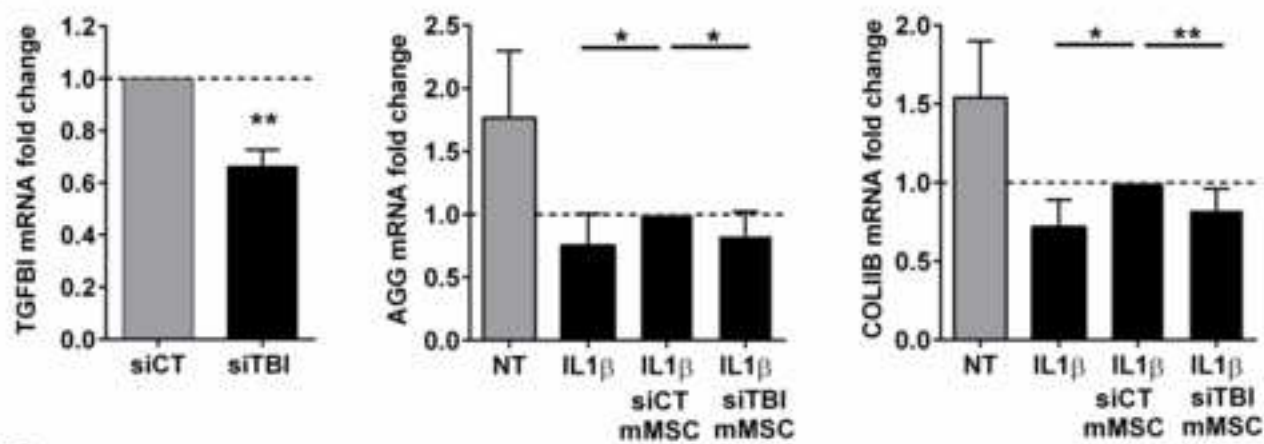


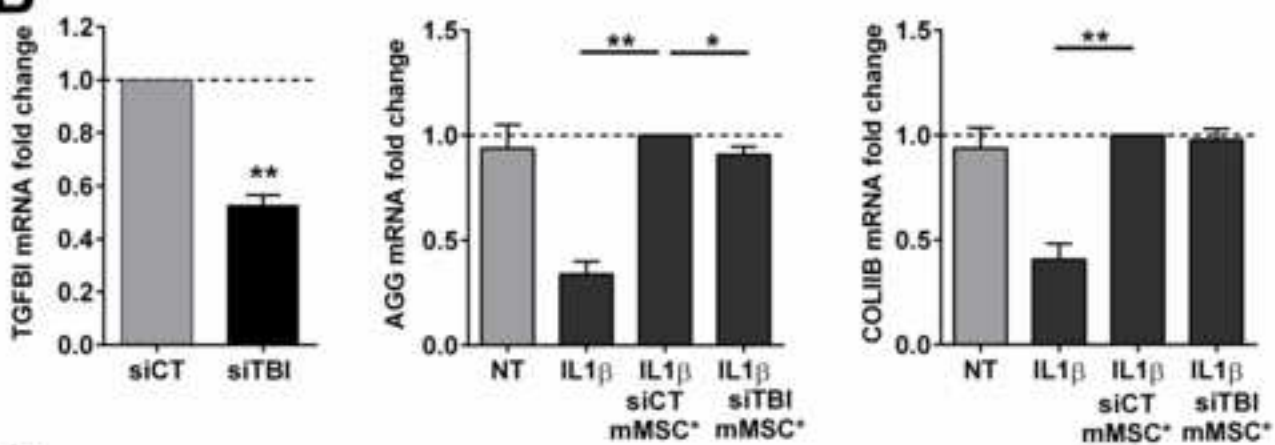
Figure 4

[Click here to download high resolution image](#)

A



B



C

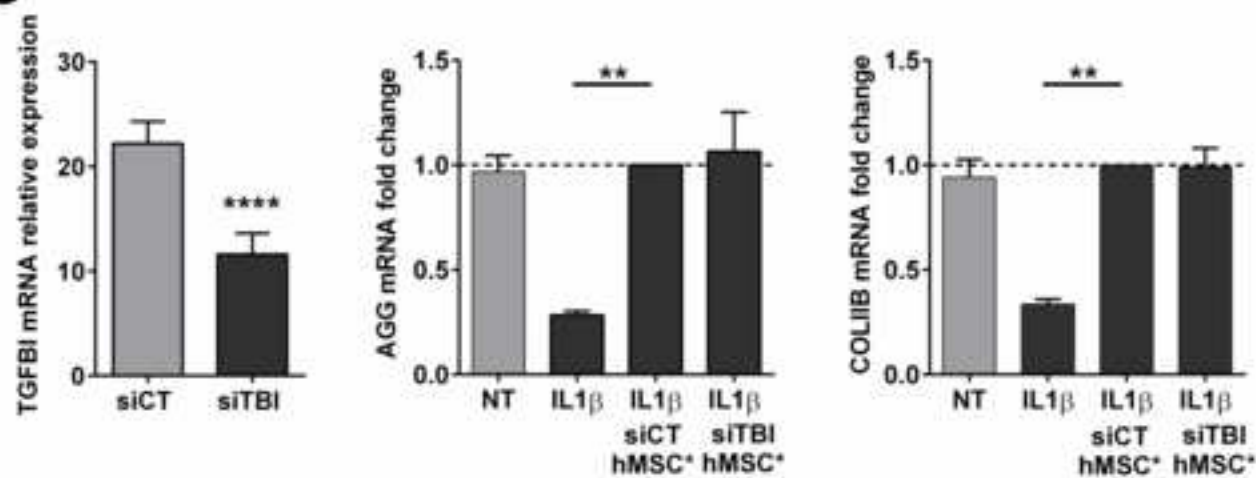


Figure 5
[Click here to download high resolution image](#)

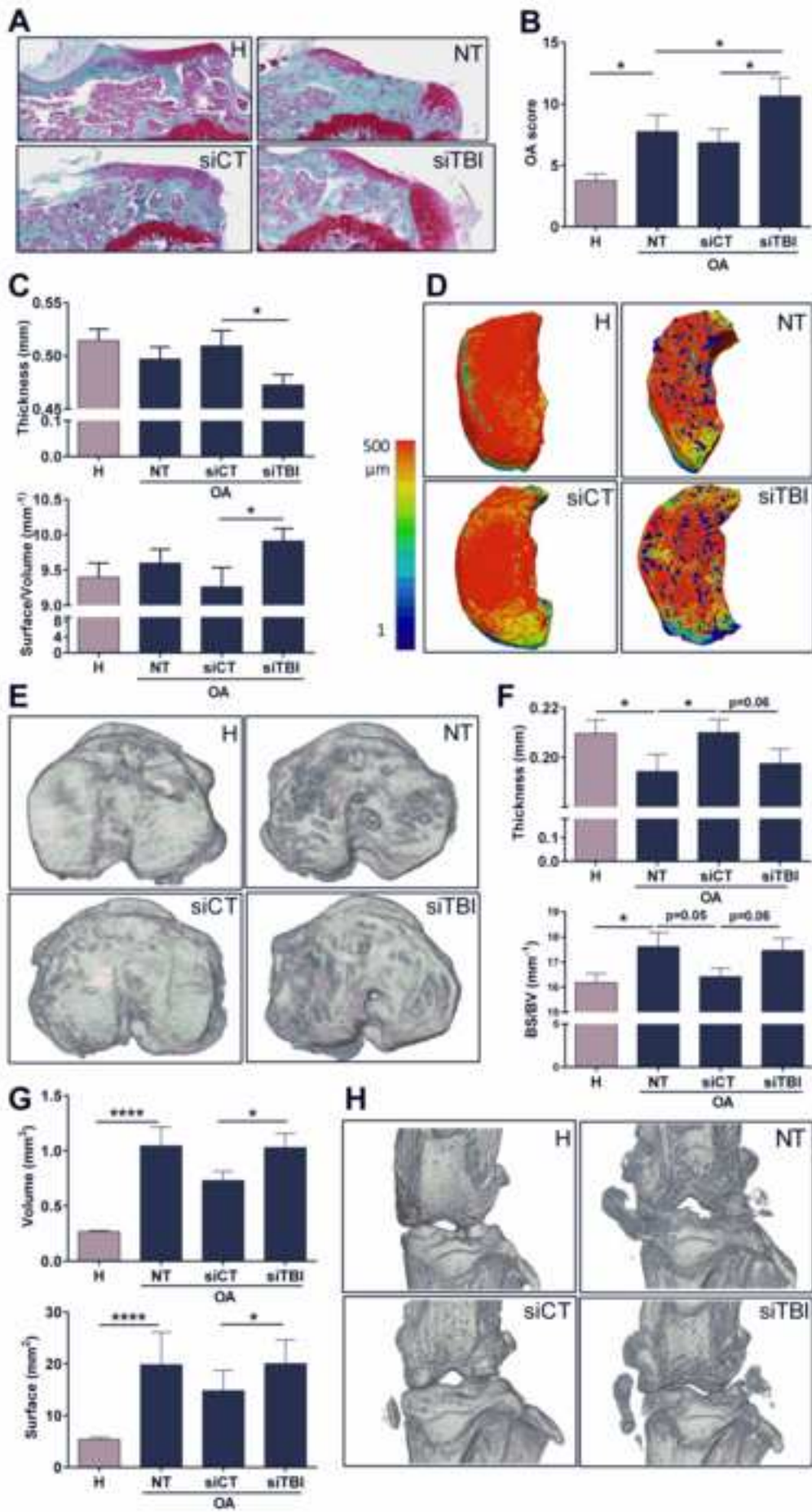


Figure 6
[Click here to download high resolution image](#)

